

1 We thank the Associate Editor for providing constructive comments to this manuscript.
2 Below we detail how we have revised the manuscript following your suggestions.

3 1. L68 (and abstract) Suggest to modify wording “inadequate [representation]” because it
4 is applied in general scope, risking to blame all available models, without mentioning that
5 the models of higher level of complexity (eg DNDC) do exist and are being applied with
6 success, although in more local, regional or site level scale.

7 *Response: Thanks for the comment. We have revised the first two sentences to “Various
8 levels of representation of biogeochemical processes in current biogeochemistry models
9 contribute to a large uncertainty in carbon budget quantification. Here, we present an
10 uncertainty analysis with a process-based biogeochemistry model, the Terrestrial
11 Ecosystem Model (TEM), that was incorporated with detailed microbial mechanisms”*

12

13 2. L112 Q10 is wrongly defined as “soil temperature (Q10)”

14 *Response: Thanks for the comment. We have modified the definition of Q_{10} as
15 “temperature sensitivity of heterotrophic soil respiration”.*

16

17 3. L125 soil temperature DT definition is vague (could be (T-273)?)

18 *Response: Thanks for the comment. We have modified the term “DT” as “temp”, which
19 is consistent with the content below. The term “temp” represents soil temperature at top
20 20 cm, and the units are °C.*

21

22 4. L144 Another temperature is defined as temp, is it different from DT?

23 *Response: Thanks for the comment. The term “temp” represents soil temperature at top
24 20 cm, and the units are °C. It is the same as previous “DT”. And we have modified the
25 term “DT” to “temp” to make them consistent.*

26

27 5. L151 Better to call r ‘rate constant’, not constant rate.

28 *Response: Thanks for the comment. We have changed r to “rate constant”.*

29

30 6. L154 Definition “rdeath and rEnzProd are the ratio of microbial death and enzyme
31 production” contradicts L151 where both are defined as “constant rates”

32 *Response: Thanks for the comment. We have changed “the ratio” to “rate constants”.*

33

34

35

36 7. L175 renzloss is defined as the ratio of enzyme loss, while it looks more like rate
37 constant

38 *Response: Thanks for the comment. We have changed r to “rate constant”.*

39

40 8. L199 need to explain factors in eq 18.

41 *Response: Thanks for the comment. We have added the explanation for factors and
42 functions “Where Cmax is the maximum rate of carbon assimilation, PAR is
43 photosynthetically active radiation, and f(phenology) represents the effects of leaf area
44 (Raich et al., 1991). The function f(foliage) represents the ratio of canopy leaf biomass
45 relative to maximum leaf biomass (Zhuang et al., 2002). T is monthly air temperature,
46 and f(CO2) represents the effects of elevated atmospheric CO2 (McGuire et al., 1997;
47 Pan et al., 1998). The function f(NA) models the limiting effects of plant nitrogen status on
48 GPP (McGuire et al., 1992; Pan et al., 1998). The function f(FT) represents the effects
49 of freeze-thaw (Zhuang et al., 2003). ”.*

50

51 9. L436 Suggest adding initials to persons name.

52 *Response: We didn’t use his data and we deleted that sentence.*

53

54 10. English should be checked carefully, especially in sections 2.2, 2.3, 3.3

55 *Response: We carefully checked English for the manuscript, especially for these sections
56 in this revision.*

1 Microbial decomposition processes and vulnerable Arctic soil organic carbon in the 21st century

2

3

4 Junrong Zha and Qianlai Zhuang

5

6 Department of Earth, Atmospheric, and Planetary Sciences and Department of Agronomy,
7 Purdue University, West Lafayette, IN 47907 USA

8

9 Submitted to: *Biogeoscience*

10 Correspondence to: qzhuang@purdue.edu

11

12

13

14

15

16

17

18

19

20

21

22

23

24

25 **Abstract**

26 Various levels of Inadequate representation of biogeochemical processes in current
27 biogeochemistry models contributes to a large uncertainty in carbon budget quantification.
28 Here, we present an uncertainty analysis with detailed microbial mechanisms were
29 incorporated into a process-based biogeochemistry model, the Terrestrial Ecosystem Model
30 (TEM), that was incorporated with detailed microbial mechanisms. Ensemble regional
31 simulations with the new model (MIC-TEM) estimated the carbon budget of the Arctic
32 ecosystems is 76.0 ± 114.8 Pg C during the 20th century, -3.1 ± 61.7 Pg C under the RCP 2.6
33 scenario and 94.7 ± 46 Pg C under the RCP 8.5 scenario during the 21st century. Positive
34 values indicate the regional carbon sink while negative values are source to the atmosphere.
35 Compared to the estimates using a simpler soil decomposition algorithm in TEM, the new
36 model estimated that the Arctic terrestrial ecosystems stored 12 Pg less carbon over the 20th
37 century, 19 Pg C and 30 Pg C less under the RCP 8.5 and RCP 2.6 scenarios, respectively,
38 during the 21st century. When soil carbon within depths 30 cm, 100 cm and 300 cm was
39 considered as initial carbon in the 21st century simulations, the region was estimated to
40 accumulate 65.4, 88.6, and 109.8 Pg C, respectively, under the RCP 8.5 scenario. In contrast,
41 under the RCP 2.6 scenario, the region lost 0.7, 2.2, and 3 Pg C, respectively, to the
42 atmosphere. We conclude that the future regional carbon budget evaluation largely
43 depends on whether or not the adequate microbial activities are represented in earth
44 system models and the sizes of soil carbon considered in model simulations.

45

46

47

48 **1. Introduction**

49 Northern high-latitude soils and permafrost contain more than 1,600 Pg carbon (Tarnocai
50 et al., 2009). Climate over this region has warmed in recent decades (Serreze and Francis, 2006)
51 and the increase is 1.5 to 4.5 times the global mean (Holland and Bitz, 2003). Warming-induced
52 changes in carbon cycling are expected to exert large feedbacks to the global climate system
53 (Davidson and Janssens, 2006; Christensen and Christensen, 2007; Oechel et al., 2000).

54 Warming is expected to accelerate soil C loss by increasing soil respiration, but
55 increasing nutrient mineralization, thereby stimulating plant net primary production (NPP)
56 (Mack et al., 2004). Thus, the variation of climate may switch the role of the Arctic system
57 between a C sink and a source if soil C loss overtakes NPP (Davidson et al., 2000; Jobbágy and
58 Jackson, 2000). Process-based biogeochemical models such as TEM (Hayes et al., 2014; Raich
59 and Schlesinger, 1992; McGuire et al., 1992; Zhuang et al., 2001, 2002, 2003, 2010, 2013),
60 Biome-BGC (Running and Coughlan, 1988), CASA (Potter et al., 1993), CENTURY (Parton et
61 al., 1994) and Biosphere Energy Transfer Hydrology scheme (BETHY) (Knorr et al., 2000) have
62 been widely used to quantify the response of carbon dynamics to climatic changes (Todd-Brown
63 et al., 2012). An ensemble of process-based model simulations suggests that arctic ecosystems
64 acted as a sink of atmospheric CO₂ in recent decades (McGuire et al., 2012; Schimel et al., 2013).
65 However, the response of this sink to increasing levels of atmospheric CO₂ and climate change is
66 still uncertain (Todd-Brown et al., 2013). The IPCC 5th report also shows that land carbon
67 storage is the largest source of uncertainty in the global carbon budget quantification (Ciais et al.,
68 2013).

69 Much of the uncertainty is also due to the relatively lower levels of inadequate
70 representation of ecosystem processes that determine the exchanges of water, energy and C
71 between land ecosystems and the atmosphere (Wieder et al., 2013), and ignorance of some key
72 biogeochemical mechanisms (Schmidt et al., 2011). For example, heterotrophic respiration (R_H)
73 is the primary loss pathway for soil organic carbon (Hanson et al., 2000; Bond-Lamberty and
74 Thomson, 2010), and it generally increases with increasing temperature (Davidson and Janssens,
75 2006) and moisture levels in well-drained soils (Cook and Orchard, 2008). Moreover, this
76 process is closely related to soil nitrogen mineralization that determines soil N availability and
77 affects gross primary production (Hao et al., 2015). To date, most models treated soil
78 decomposition as a first-order decay process, i.e., CO_2 respiration is directly proportional to soil
79 organic carbon. However, it is not clear if these models are robust under changing environmental
80 conditions (Lawrence et al., 2011; Schimel and Weintraub, 2003; Barichivich et al., 2013) since
81 they often ignored the effects of changes in biomass and composition of decomposers, while
82 recent empirical studies have shown that microbial abundance and community play a significant
83 role in soil carbon decomposition (Allison and Martiny, 2008). The control that microbial activity
84 and enzymatic kinetics imposed on soil respiration suggests the need for explicit representation
85 of microbial physiology, enzymatic activity, in addition to the direct effects of soil temperature
86 and soil moisture on heterotrophic respiration (Schimel and Weintraub, 2003). Recent
87 mechanistically-based models explicitly incorporated with the microbial dynamics and enzyme
88 kinetics that catalyze soil C decomposition have produced notably different results and a closer
89 match to contemporary observations (Wieder et al., 2013; Allison et al., 2010) indicating the need

90 for incorporating these microbial mechanisms into large-scale earth system models to quantify
91 carbon dynamics under future climatic conditions ((Wieder et al., 2013; Allison et al., 2010).

92 This study advanced a microbe-based biogeochemistry model (MIC-TEM) based on an
93 extant Terrestrial Ecosystem Model (TEM) (Raich and Schlesinger, 1992; McGuire et al., 1992;
94 Zhuang et al., 2001, 2002, 2003, 2010, 2013; Hao et al., 2015). In MIC-TEM, the heterotrophic
95 respiration is not only a function of soil temperature, soil organic matter (SOM) and soil
96 moisture, but also considers the effects of dynamics of microbial biomass and enzyme kinetics
97 (Allison et al., 2010). The verified MIC-TEM was used to quantify the regional carbon dynamics
98 in northern high latitudes (north 45 °N) during the 20th and 21st centuries.

99

100 **2. Methods**

101 **2.1 Overview**

102 Below we first briefly describe how we advanced the MIC-TEM by modifying the soil
103 respiration process in TEM (Zhuang et al., 2003) to better represent carbon dynamics in
104 terrestrial ecosystems. Second, we describe how we parameterized and verified the new model
105 using observed net ecosystem exchange data at representative sites and how simulated net
106 primary productivity (NPP) was evaluated with Moderate Resolution Imaging Spectroradiometer
107 (MODIS) data to demonstrate the reliability of new model at regional scales. Third, we present
108 how we applied the model to the northern high latitudes for the 20th and 21st centuries. Finally,
109 we introduce how we conducted the sensitivity analysis on initial soil carbon input, using
110 gridded observation-based soil carbon data of three soil depths during the 21st century.

111

112 **2.2 Model description**

113 TEM is a highly aggregated large-scale biogeochemical model that estimates the dynamics of
114 carbon and nitrogen fluxes and pool sizes of plants and soils using spatially y-explicit referenced
115 information on climate, elevation, soils and vegetation ([Raich and Schlesinger, 1992](#); McGuire et
116 al., 1992; Zhuang et al., 2003, 2010; Melillo et al., 1993). To explicitly consider the effects of
117 microbial dynamics and enzyme kinetics on large-scale carbon dynamics of northern terrestrial
118 ecosystems, we developed MIC-TEM by coupling version 5.0 of TEM (Zhuang et al., 2003,
119 2010) with a microbial-enzyme module (Hao et al., 2015; Allison et al., 2010). Our modification
120 of the TEM improved the representation of the heterotrophic respiration (R_H) from a first-order
121 structure to a more detailed structure (Fig. S1).

122 In TEM, heterotrophic respiration R_H is calculated as a function of soil organic carbon
123 (SOC), soil temperature temperature sensitivity of heterotrophic soil respiration (Q_{10}), soil
124 moisture ($f(MOIST)$), and the gram-specific decomposition constant K_d :

$$125 R_H = K_d * SOC * Q_{10}^{\frac{temp}{10}} * f(MOIST) \quad (1)$$

126 Where temp is soil temperature at top 20 cm (units: °C). CO₂ production from SOC pool is
127 directly proportional to the pool size, and the activity of decomposers only depends on the built-
128 in relationships with soil temperature and moisture (Todd-Brown et al., 2012). Therefore, the
129 changes in microbial community composition or adaption of microbial physiology to new
130 conditions were not represented in TEM. However, current studies indicate that soil C
131 decomposition depends on the activity of biological communities dominated by microbes
132 (Schimel and Weintraub, 2003), implying that the biomass and composition of the decomposer
133 community can't be ignored (Todd-Brown et al., 2012).

134 We thus revised the first-order soil C structure in TEM to a second-order structure
135 considering microbial dynamics and enzyme kinetics according to Allison et al. (2010). In MIC-
136 TEM, heterotrophic respiration (R_H) is calculated as:

137
$$R_H = ASSIM * (1 - CUE) \quad (2)$$

138 Where ASSIM and CUE represent microbial assimilation and carbon use efficiency, respectively.
139 ASSIM is modeled with a Michaelis-Menten function:

140
$$ASSIM = V_{max_{uptake}} * MIC * \frac{DOC}{K_{m_{uptake}} + DOC} \quad (3)$$

141 Where DOC is dissolved organic carbon and $V_{max_{uptake}}$ is the maximum velocity of the
142 reaction and calculated using the Arrhenius equation:

143
$$V_{max_{uptake}} = V_{max_{uptake_0}} * e^{\frac{Ea_{uptake}}{R * (temp + 273)}} \quad (4)$$

144 where $V_{max_{uptake_0}}$ is the pre-exponential coefficient, Ea_{uptake} is the activation energy for the
145 reaction ($Jmol^{-1}$), R is the gas constant ($8.314 Jmol^{-1}K^{-1}$), and temp is the temperature in Celsius
146 under the reaction occurs. Here we used soil temperature at top 20 cm.

147 Besides, $K_{m_{uptake}}$ value is calculated as a linear function of temperature:

148
$$K_{m_{uptake}} = K_{m_{uptake_{slope}}} * temp + K_{m_{uptake_0}} \quad (5)$$

149 Microbial biomass MIC is modeled as:

150
$$\frac{dMIC}{dt} = ASSIM * CUE - DEATH - EPROD \quad (6)$$

151 Where microbial biomass death (DEATH) and enzyme production (EPROD) are modeled as
152 proportional to microbial biomass with rate constants-constant rates r_{death} and $r_{EnzProd}$:

153
$$DEATH = r_{death} * MIC \quad (7)$$

154
$$EPROD = r_{EnzProd} * MIC \quad (8)$$

155 Where r_{death} and r_{EnzProd} are the rate constantsratio of microbial death and enzyme production,
156 respectively.

157 DOC is part of soil organic carbon:

158
$$\frac{d\text{DOC}}{dt} = \text{DEATH} * (1 - \text{MICtoSOC}) + \text{DECAY} + \text{ELOSS} - \text{ASSIM} \quad (9)$$

159 where MICtoSOC is carbon input ratio as dead microbial biomass to SOC, representing the
160 fraction of microbial death that flows into SOC, and is set as a constant value according to
161 Allison et al. (2010). SOC dynamics are modeled:

162
$$\frac{d\text{SOC}}{dt} = \text{Litterfall} + \text{DEATH} * \text{MICtoSOC} - \text{DECAY} \quad (10)$$

163 Where Litterfall is estimated as a function of vegetation carbon (Zhuang et al., 2010). The
164 enzymatic decay of SOC is calculated as:

165
$$\text{DECAY} = V_{\text{max}} * \text{ENZ} * \frac{\text{SOC}}{K_m + \text{SOC}} \quad (11)$$

166 Where V_{max} is the maximum velocity of the reaction and calculated using the Arrhenius equation:

167
$$V_{\text{max}} = V_{\text{max}_0} * e^{\frac{Ea}{R * (\text{temp} + 273)}} \quad (12)$$

168 The parameters Km and carbon use efficiency (CUE) are temperature sensitive, and calculated
169 as a linear function of temperature between 0 and 50°C:

170
$$K_m = K_{m_{\text{slope}}} * \text{temp} + K_{m_0} \quad (13)$$

171
$$\text{CUE} = \text{CUE}_{\text{slope}} * \text{temp} + \text{CUE}_0 \quad (14)$$

172 Where CUESlope and CUE_0 are parameters for calculating CUE, and $K_{m_{\text{slope}}}$ and K_{m_0} are
173 parameters for calculating Km. The values of $\text{CUE}_{\text{slope}}$, CUE_0 , $K_{m_{\text{slope}}}$, and K_{m_0} were derived
174 from Allison et al. (2010).

175 ELOSS is also a first-order process, representing the loss of enzyme:

176 $ELOSS = r_{enzloss} * ENZ$ (15)

177 Where $r_{enzloss}$ is the rate constant of enzyme loss. Enzyme pool (ENZ) is modeled:

178 $\frac{dENZ}{dt} = EPORD - ELOSS$ (16)

179 Heterotrophic respiration (R_H) is an indispensable component of soil respiration (Bond-
180 Lamberty and Thomson, 2010), and closely coupled with soil nitrogen (N) mineralization that
181 determines soil N availability, affecting gross primary production (GPP).

182

183

184 **2.3 Model parameterization and validation**

185 The variables and parameters of these microbial dynamics and their impacts on soil C
186 decomposition were detailed in Allison et al. (2010) (Table 1). Here we parameterized MIC-
187 TEM for representative ecosystem types in northern high latitudes based on monthly net
188 ecosystem production on site (NEP, $gCm^{-2} mon^{-1}$) measurements from AmeriFlux network
189 (Davidson et al., 2000) (Table S1). The results for model parameterization were presented in
190 Fig. S2. Another set of level 4 gap-filled NEP data was used for model validation at site level
191 (Table S2). The site-level monthly climate data of air temperature ($^{\circ}C$), precipitation (mm) and
192 cloudiness (%) were used to drive the model. Gridded MODIS NPP data from 2001 to 2010 were
193 used to evaluate regional NPP simulations. The MODIS NPP data was developed by the MOD17
194 MODIS project. The product name is Net Primary Production Yearly L4 Global 1 km. The
195 critical parameter used in MOD17 algorithm is conversion efficiency parameter ϵ . More
196 information about the MODIS NPP product can be found at
197 https://neo.sci.gsfc.nasa.gov/view.php?datasetId=MOD17A2_M_PSN.

198 In TEM, NPP is calculated as:

199
$$\mathbf{NPP}=\mathbf{GPP}-\mathbf{R}_A \quad (17)$$

200 Where GPP is gross primary production, and R_A is autotrophic respiration. [GPP is defined as:](#)

201
$$GPP = C_{max} * f(PAR) * f(phenology) * f(foliage) * f(T) * f(CO_2) * f(NA) * f(FT) \quad (18)$$

202 [Where \$C_{max}\$ is the maximum rate of carbon assimilation, PAR is photosynthetically active](#)
203 [radiation, and \$f\(phenology\)\$ represents the effects of leaf area \(Raich et al., 1991\). The function](#)
204 [\$f\(foliage\)\$ represents the ratio of canopy leaf biomass relative to maximum leaf biomass \(Zhuang](#)
205 [et al., 2002\). T is monthly air temperature, and \$f\(CO_2\)\$ represents the effects of elevated](#)
206 [atmospheric CO₂ \(McGuire et al., 1997; Pan et al., 1998\). The function \$f\(NA\)\$ models the limiting](#)
207 [effects of plant nitrogen status on GPP \(McGuire et al., 1992; Pan et al., 1998\). The function \$f\$](#)
208 [\(FT\) represents the effects of freeze-thaw \(Zhuang et al., 2003; Tian et al., 1999\).](#)

209 For detailed GPP and R_A calculations, see Zhuang et al. (2003).

210 The parameterization was conducted with a global optimization algorithm SCE-UA (Shuffled
211 complex evolution) (Duan et al., 1994) to minimize the difference between the monthly
212 simulated and measured NEE at these sites (Fig. S2). The cost function of the minimization is:

213
$$Obj = \sum_{i=1}^k (NEP_{obs,i} - NEP_{sim,i})^2 \quad (19)$$

214 Where $NEP_{obs,i}$ and $NEP_{sim,i}$ are the observed and simulated NEP, respectively. k is the number
215 of data pairs for comparison. Other parameters used in MIC-TEM were default values from TEM
216 5.0 (Zhuang et al., 2003, 2010). The optimized parameters were used for model validation and
217 regional extrapolations.

218

219 **2.4 Regional simulations**

220 Two sets of regional simulations for the 20th century using MIC-TEM and TEM at a spatial
221 resolution of 0.5° latitude × 0.5° longitude were conducted. Gridded forcing data of monthly air
222 temperature, precipitation, and cloudiness were used, along with other ancillary inputs including
223 historical atmospheric CO₂ concentrations, soil texture, elevation, and potential natural
224 vegetation. Climatic inputs vary over time and space, whereas soil texture, elevation, and land
225 cover data are assumed to remain unchanged throughout the 20th century, which only vary
226 spatially. The transient climate data during the 20th century was organized from the Climatic
227 Research Unit (CRU TS3.1) from the University of East Anglia (Harris et al., 2014). The
228 spatially-explicit data include potential natural vegetation (Melillo et al., 1993), soil texture
229 (Zhuang et al., 2003) and elevation (Zhuang et al., 2015).

230 Similarly, two sets of simulations were conducted driven with two contrasting climate
231 change scenarios (RCP 2.6 and RCP 8.5) over the 21st century. The future climate change
232 scenarios were derived from the HadGEM2-ES model, which is a member of CMIP5 project
233 (<https://esgf-node.llnl.gov/search/cmip5/>). The future atmospheric CO₂ concentrations and
234 climate forcing from each of the two climate change scenarios were used. The simulated NPP, R_H
235 and NEP by both models (TEM 5.0 and MIC-TEM) were analyzed. The positive NEP represents
236 a CO₂ sink from the atmosphere to terrestrial ecosystems, while a negative value represents a
237 source of CO₂ from terrestrial ecosystems to the atmosphere.

238 Besides, in order to test the parameter uncertainty in our model, we conducted the
239 regional simulations with 50 sets of parameters for both historical and future studies. The 50 sets

240 of parameters were obtained according to the method in Tang and Zhuang (2008). The upper and
241 lower bounds of the regional estimations were generated based on these simulations.

242

243 **2.5 Sensitivity to initial soil carbon input**

244 Future carbon dynamics can be affected by varying initial soil carbon amount. In the standard
245 simulation of TEM, the initial soil carbon amount for transient simulations was obtained from
246 equilibrium and spin-up periods directly for each grid cell in the region. To test the sensitivity to
247 the initial soil carbon amount in transient simulations for the 21st century, we used empirical soil
248 organic carbon data extracted from the Northern Circumpolar Soil Carbon Database (NCSCD)
249 (Tarnocai et al., 2009), as the initial soil carbon amount. The 0.5° × 0.5° soil carbon data
250 products for three different depths of 30cm, 100cm and 300cm were used. The sensitivity test
251 was conducted for transient simulations under the RCP 2.6 and RCP 8.5 scenarios. To avoid the
252 instability of C-N ratio caused by replacing the initial soil carbon pool with observed data at the
253 beginning of transient period, initial soil nitrogen values were also generated based on the soil
254 carbon data and corresponding C-N ratio map for transient simulations (Zhuang et al., 2003;
255 Raich and Schlesinger, 1992).

256

257 **3. Results**

258 **3.1 Model verification at site and regional levels**

259 With the optimized parameters, MIC-TEM reproduces the carbon dynamics well for alpine
260 tundra, boreal forest, temperate coniferous forest, temperate deciduous forest, grasslands and wet
261 tundra with R^2 ranging from 0.70 for Ivotuk to 0.94 for Bartlett Experimental Forest (Fig. S3,

262 table S3). In general, model performs better for forest ecosystems than for tundra ecosystems.
263 The temporal NPP from 2001 to 2010 simulated by MIC-TEM and TEM were compared with
264 MODIS NPP data (Fig. S4). Pearson correlation coefficients are 0.52 (MIC-TEM and MODIS)
265 and 0.34 (TEM and MODIS). NPP simulated by MIC-TEM showed higher spatial correlation
266 coefficients with MODIS data than TEM (Fig. S5). By considering more detailed microbial
267 activities, the heterotrophic respiration is more adequately simulated using the MIC-TEM. The
268 simulated differences in soil decomposition result in different levels of soil available nitrogen,
269 which influences the nitrogen uptake by plants, the rate of photosynthesis and NPP. The spatial
270 correlation coefficient between NPP simulated by MIC-TEM and MODIS is close to 1 in most
271 study areas, suggesting the reliability of MIC-TEM at the regional scale.

272

273 **3.2 Regional carbon dynamics during the 20th century**

274 The equifinality of the parameters in MIC-TEM was considered in our ensemble regional
275 simulations to measure the parameter uncertainty (Tang and Zhuang, 2008). Here and below, the
276 ensemble means and the inter-simulation standard deviations are shown for uncertainty measure,
277 unless specified as others. These ensemble simulations indicated that the northern high latitudes
278 act from a carbon source of 38.9 Pg_C to a carbon sink of 190.8 Pg_C by different ensemble
279 members, with the mean of 64.2±21.4 Pg at the end of 20th century while the simulation with the
280 optimized parameters estimates a regional carbon sink of 77.6 Pg with the interannual standard
281 deviation of 0.21 Pg_C yr⁻¹ during the 20th century (Fig 1). Simulated regional NEP with
282 optimized parameters using TEM and MIC-TEM showed an increasing trend throughout the 20th
283 century except a slight decrease during the 1960s (Fig. 2). The Spatial distributions of NEP

284 simulated by MIC-TEM for different periods in [the](#) 20th century also show the increasing trend
285 (Fig 3). Positive values of NEP represent sinks of CO₂ into terrestrial ecosystems, while negative
286 values represent sources of CO₂ to the atmosphere. From 1900 onwards, both models estimated a
287 regional carbon sink during the 20th century. With optimized parameters, TEM estimated higher
288 NPP and R_H at 0.6 PgC yr⁻¹ and 0.3 PgC yr⁻¹ than MIC-TEM, respectively, at the end of the 20th
289 century (Fig. 2). The MIC-TEM estimated a carbon sink increase from 0.64 to 0.83 PgCyr⁻¹
290 during the century while the estimated increase by TEM was much higher (0.28 PgCyr⁻¹) (Fig. 2).
291 At the end of the century, MIC-TEM estimated NEP reached 1.0 PgCyr⁻¹ in comparison with
292 TEM estimates of 0.3 PgCyr⁻¹. TEM estimated NPP and R_H are 0.5 Pg_Cyr⁻¹ and 0.3 Pg_C_yr⁻¹
293 higher, respectively. As a result, TEM estimated that the region accumulated 11.4 Pg more
294 carbon than MIC-TEM. Boreal forests are a major carbon sink at 0.55 and 0.63 Pg_C_yr⁻¹
295 estimated by MIC-TEM and TEM, respectively. Alpine tundra contributes the least sink. Overall,
296 TEM overestimated the sink by 12.5% in comparison to MIC-TEM for forest ecosystems and
297 16.7% for grasslands. For wet tundra and alpine tundra, TEM overestimated about 20% and 33%
298 in comparison with MIC-TEM, respectively (Table 2).

299

300 **3.3 Regional carbon dynamics during the 21st century**

301 [Simulated r](#)Regional annual NPP and R_H increases under the RCP 8.5 scenario [according to](#)
302 [simulations](#) with both models (Fig. 4). With optimized parameters, MIC-TEM estimated NPP
303 increases from 9.2 in the 2000s to 13.2 PgCyr⁻¹ in the 2090s, while TEM-predicted NPP is 2.0
304 Pg_C_yr⁻¹ higher in the 2000s and 0.3 Pg_C_yr⁻¹ higher in the 2090s (Fig. 4). Similarly, TEM also
305 overestimated R_H by 1.7 Pg_C_yr⁻¹ in the 2000s and 0.25 Pg_C_yr⁻¹ higher in the 2090s,

306 respectively (Fig. 4). As a result, the regional sink increases from 0.53 Pg C yr^{-1} in the 2000s, 1.4
307 Pg C yr^{-1} in the 2070s, then decreases to 1.1 Pg C yr^{-1} in the 2090s estimated by MIC-TEM (Fig.
308 4). Given the uncertainty in parameters, MIC-TEM predicted the region acts as a carbon sink
309 ranging from 48.7 to 140.7 Pg, with the mean of 71.7 ± 26.6 Pg at the end of 21st century, while
310 the simulation with optimized parameters estimates a regional carbon source of 79.5 Pg with the
311 interannual standard deviation of 0.37 Pg C yr^{-1} during the 21st century (Fig 4). TEM predicted a
312 similar trend for NEP, which overestimated the carbon sink with magnitude of 19.2 Pg compared
313 with the simulation by MIC-TEM with optimized parameters. Under the RCP 2.6 scenario (Fig.
314 4), the increase of NPP and R_H is smaller from 2000 to 2100 compared to the simulation under
315 the RCP 8.5. MIC-TEM predicted that NPP increases from 9.1 to 10.9 Pg C yr^{-1} , TEM estimated
316 1.6 Pg C yr^{-1} higher at the beginning and 0.9 Pg C yr^{-1} higher in the end of the 21st century (Fig.
317 4). Consequently, MIC-TEM predicted NEP fluctuates between sinks and sources during the
318 century, with a neutral before 2070, and a source between -0.2 - -0.3 Pg C yr^{-1} after the 2070s.
319 As a result, the region acts as a carbon source of 1.6 Pg C with the interannual standard deviation
320 of 0.24 Pg C yr^{-1} estimated with MIC-TEM and a sink of 27.6 Pg C with the interannual
321 standard deviation of 0.2 Pg C yr^{-1} estimated with TEM during the century (Fig. 4). When
322 considering the uncertainty source of parameters, MIC-TEM predicted the region acts from a
323 carbon source of 64.8 Pg C to a carbon sink of 58.6 Pg C during the century with the mean of -
324 3.3 \pm 20.3 Pg at the end of 21st century (Fig 4).

325

326 **3.4 Model sensitivity to initial soil carbon**

327 Under the RCP 2.6, without replacing the initial soil carbon with inventory-based estimates
328 ([Tarnocai et al., 2009](#))⁺ in model simulations, TEM estimated that the regional soil organic
329 carbon (SOC) is 604.2 Pg C and accumulates 12.1 Pg C during the 21st century. When using
330 estimated soil carbon ([Tarnocai et al., 2009](#)),⁺ within depths of 30cm, 100cm and 300cm as
331 initial pools in simulations, TEM predicted that regional SOC is 429.5, 689.3 and 1003.4 Pg C in
332 2000, and increases by 9.9, 16.0 and 22.8 Pg C at the end of the 21st century, and the regional
333 cumulative carbon sink is 20.4, 34.0, and 48.1 Pg C, respectively during the century. In contrast,
334 using the same inventory-based SOC estimates, MIC-TEM projected that the region acts from a
335 cumulative carbon sink to a source at 0.7, 2.2, and 3.0 Pg C, respectively. Under the RCP 8.5,
336 both models predicted that the region acts as a carbon sink, regardless of the magnitudes of
337 initial soil carbon pools used, with TEM projected sink of 71.7, 120, and 155.6 Pg C and a much
338 smaller cumulative sink of 65.4, 88.6, and 109.8 Pg C estimated with MIC-TEM, respectively
339 (Table 3).

340 **4. Discussion**

341 During the last few decades, a greening accompanying warming and rising atmospheric
342 CO₂ in the northern high latitudes (>45° N) has been documented (McGuire et al., 1995;
343 McGuire and Hobbie, 1997; Chapin and Starfield, 1997; Stow et al., 2004; Callaghan et al., 2005;
344 Tape et al., 2006). The large stocks of carbon contained in the region (Tarnocai et al., 2009) are
345 particularly vulnerable to climate change (Schuur et al., 2008; McGuire et al., 2009). To date, the
346 degree to which the ecosystems may serve as a source or a sink of C in the future are still
347 uncertain (McGuire et al., 2009; Wieder et al., 2013). Therefore, accurate models are essential for
348 predicting carbon–climate feedbacks in the future (Todd-Brown et al., 2013). Our regional

349 simulations indicate the region is currently a carbon sink, which is consistent with many previous
350 studies (White et al., 2000; Houghton et al., 2007), and this sink will grow under the RCP 8.5
351 scenario, but shift to a carbon source under the RCP 2.6 scenario by 2100. MIC-TEM shows a
352 higher correlation between NPP and soil temperature ($R=0.91$) than TEM ($R=0.82$), suggesting
353 that MIC-TEM is more sensitive to environmental changes (Table S4).

354 Our regional estimates of carbon fluxes by MIC-TEM are within the uncertainty range
355 from other existing studies. For instance, Zhuang et al. (2003) estimated the region as a sink of
356 0.9 Pg C yr^{-1} in extratropical ecosystems for the 1990s, which is similar to our estimation of 0.83
357 Pg C yr^{-1} by MIC-TEM. White et al. (2000) estimated that, during the 1990s, regional NEP
358 above 50°N region is $0.46 \text{ Pg C yr}^{-1}$ while Qian et al. (2010) estimated that NEP increased from
359 0 to 0.3 Pg C yr^{-1} for the high-latitude region above 60°N during last century, and reached 0.25
360 Pg C yr^{-1} during the 1990s. White et al. (2000) predicted that, from 1850 to 2100, the region
361 accumulated 134 Pg C in terrestrial ecosystems, in comparison with our estimates of 77.6 Pg C
362 with MIC-TEM and 89 Pg C with TEM. Our projection of a weakening sink during the second
363 half of the 21st century is consistent with previous model studies (Schaphoff et al., 2013). Our
364 predicted trend of NEP is very similar to the finding of White et al. (2000), indicating that NEP
365 increases from $0.46 \text{ Pg C yr}^{-1}$ in the 2000s and reaches 1.5 Pg C yr^{-1} in the 2070s, then decreases
366 to 0.6 Pg C yr^{-1} in the 2090s.

367 The MIC-TEM simulated NEP generally agrees with the observations. However, model
368 simulations still deviate from the observed data, especially for tundra ecosystems. The deviation
369 may be due to the uncertainty or errors in the observed data, which do not well constrain the
370 model parameters. Uncertain driving data such as temperature and precipitation are also a source

371 of uncertainty for transient simulations. In addition, we assumed that vegetation will not change
372 during the transient simulation. However, over the past few decades in the northern high latitudes,
373 temperature increases have led to vegetation changes (Hansen et al., 2006), including latitudinal
374 treeline advance (Lloyd et al., 2005) and increasing shrub density (Sturm et al., 2001). Vegetation
375 can shift from one type to another because of competition for light, N and water (White et al.,
376 2000). For example, needleleaved trees tend to replace tundra gradually in response to warming.
377 In some areas, forests even moved several hundreds of kilometers within 100 years (Gear and
378 Huntley, 1991). The vegetation changes will affect carbon cycling in these ecosystems. In
379 addition, we have not yet considered the effects of management of agriculture lands (Cole et al.,
380 1997), but Zhuang et al. (2003) showed that the changes in agricultural land use in northern high
381 latitudes have been small.

382 The largest limitation to this study is that we have not explicitly considered the fire
383 effects. Warming in the northern high latitudes could favor fire in its frequency, intensity,
384 seasonality and extent (Kasischke and Turetsky, 2006; Johnstone and Kasischke, 2005; Soja et al.,
385 2007; Randerson et al., 2006; Bond-Lamberty et al., 2007). Fire has profound effects on northern
386 forest ecosystems, altering the N cycle and water and energy exchanges between the atmosphere
387 and ecosystems. Increase in wildfires will destroy most of above-ground biomass and consume
388 organic soils, resulting in less carbon uptake by vegetation (Harden et al., 2000), leading to a net
389 release of carbon in a short term. However, a suite of biophysical mechanisms of ecosystems
390 including post-fire increase in the surface albedo and rates of biomass accumulation may in turn,
391 exert a negative feedback to climate warming (Amiro et al., 2006; Goetz et al., 2007), further
392 influence the carbon exchanges between ecosystems and the atmosphere.

393 Moreover, carbon uptake in land ecosystems depends on new plant growth, which
394 connects tightly with the availability of nutrients such as mineral nitrogen. Recent studies have
395 shown that when soil nitrogen is in short supply, most terrestrial plants would form symbiosis
396 relationships with fungi; hyphae provides nitrogen to plants, in return, plants provide sugar to
397 fungi (Hobbie and Hobbie, 2008, 2006; Schimel and Hättenschwiler, 2007). This symbiosis
398 relationship has not been considered in our current modeling, which may lead to a large
399 uncertainty in our quantification of carbon and nitrogen dynamics.

400 Shift in microbial community structure was not considered in our model, which could
401 affect the temperature sensitivity of heterotrophic respiration (Stone et al., 2012). Michaelis-
402 Menten constant (K_m) could also adapt to climate warming, and it may increase more
403 significantly with increasing temperature in cold-adapted enzymes than in warm-adapted
404 enzymes (German et al., 2012; Somero et al., 2004; Dong and Somero, 2009). Carbon use
405 efficiency (CUE) is also a controversial parameter in our model. Empirical studies in soils
406 suggest that microbial CUE declines by at least $0.009\text{ }^{\circ}\text{C}^{-1}$ (Steinweg et al., 2008), while other
407 studies find that CUE is invariant with temperature (López-Urrutia and Morán, 2007). Another
408 key microbial trait lacking in our modeling is microbial dormancy (He et al., 2015). Dormancy is
409 a common, bet-hedging strategy used by microorganisms when environmental conditions limit
410 their growth and reproduction (Lennon and Jones, 2011). Microorganisms in dormancy are not
411 able to drive biogeochemical processes such as soil CO_2 production, and therefore, only active
412 microorganisms should be involved in utilizing substrates in soils (Blagodatskaya and Kuzyakov,
413 2013). Many studies have indicated that soil respiration responses to environmental conditions
414 are more closely associated with the active portion of microbial biomass than total microbial

415 biomass (Hagerty et al., 2014; Schimel and Schaeffer, 2012; Steinweg et al., 2013). Thus, the
416 ignorance of microbial dormancy could fail to distinguish microbes with different physiological
417 states, introducing uncertainties to our carbon estimation.

418 **5. Conclusions**

419 This study used a more detailed microbial biogeochemistry model to investigate the carbon
420 dynamics in the region for the past and this century. Regional simulations using MIC-TEM
421 indicated that, over the 20th century, the region is a sink of 77.6 Pg [C](#). This sink could reach to
422 79.5 Pg [C](#) under the RCP 8.5 scenario or shift to a carbon source of 1.6 Pg under the RCP 2.6
423 scenario during [the](#) 21st century. On the other hand, traditional TEM overestimated the carbon
424 sink under the RCP 8.5 scenario with magnitude of 19.2 Pg than MIC-TEM, and predicted this
425 region acting as [a](#) carbon sink with magnitude of 27.6 Pg under the RCP 2.6 scenario during [the](#)
426 21st century. Using recent soil carbon stock data as initial soil carbon in model simulations, the
427 region was estimated to shift from a carbon sink to a source, with total carbon release at 0.7- 3
428 Pg by 2100 depending on initial soil carbon pools at different soil depths under the RCP 2.6
429 scenario. In contrast, the region acts as a carbon sink at 55.4 - 99.8 Pg [C](#) in the 21st century under
430 [the](#) RCP 8.5 scenario. Without considering more detailed microbial processes, models estimated
431 that the region acts as a carbon sink under both scenarios. Under the RCP 2.6 scenario, the
432 cumulative sink ranges from 9.9 to 22.8 Pg C. Under the RCP 8.5 scenario, the cumulative sink
433 is even larger at 71.7 - 155.6 Pg C. This study indicated that more detailed microbial
434 physiology-based biogeochemistry models estimate carbon dynamics very differently from using
435 a relatively simple microbial decomposition-based model. The comparison with satellite

436 products or other estimates for the 20th century suggests that the more detailed microbial
437 decomposition shall be considered to adequately quantify C dynamics in northern high latitudes.

438

439

440 **Acknowledgments**

441 This research was supported by a NSF project (IIS-1027955), a DOE project (DE-SC0008092),
442 and a NASA LCLUC project (NNX09AI26G) to Q. Z. We acknowledge the Rosen High
443 Performance Computing Center at Purdue for computing support. We thank the National Snow
444 and Ice Data center for providing Global Monthly EASE-Grid Snow Water Equivalent data,
445 National Oceanic and Atmospheric Administration for North American Regional Reanalysis
446 (NARR). ~~, and G. Hugelius and his group by making available pan-Arctic permafrost soil C~~
447 ~~maps~~. We also acknowledge the World Climate Research Programme's Working Group on
448 Coupled Modeling Intercomparison Project CMIP5, and we thank the climate modeling groups
449 for producing and making available their model output. The data presented in this paper can be
450 accessed through our research website (<http://www.eaps.purdue.edu/ebdl/>)

451

452 **References**

453 Allison, S. D., and Martiny, J. B.: Colloquium paper: resistance, resilience, and redundancy in
454 microbial communities, Proceedings of the National Academy of Sciences of the United States
455 of America, 105 Suppl 1, 11512-11519, 10.1073/pnas.0801925105, 2008.
456 Allison, S. D., Wallenstein, M. D., and Bradford, M. A.: Soil-carbon response to warming
457 dependent on microbial physiology, Nature Geoscience, 3, 336-340, 10.1038/ngeo846, 2010.

458 Amiro, B. D., Orchansky, A. L., Barr, A. G., Black, T. A., Chambers, S. D., Chapin III, F. S.,
459 Goulden, M. L., Litvak, M., Liu, H. P., McCaughey, J. H., McMillan, A., and Randerson, J. T.:
460 The effect of post-fire stand age on the boreal forest energy balance, *Agricultural and Forest
461 Meteorology*, 140, 41-50, 10.1016/j.agrformet.2006.02.014, 2006.

462 Barichivich, J., Briffa, K. R., Myneni, R. B., Osborn, T. J., Melvin, T. M., Ciais, P., Piao, S., and
463 Tucker, C.: Large-scale variations in the vegetation growing season and annual cycle of
464 atmospheric CO₂ at high northern latitudes from 1950 to 2011, *Global change biology*, 19, 3167-
465 3183, 10.1111/gcb.12283, 2013.

466 Blagodatskaya, E., and Kuzyakov, Y.: Active microorganisms in soil: Critical review of
467 estimation criteria and approaches, *Soil Biology and Biochemistry*, 67, 192-211,
468 10.1016/j.soilbio.2013.08.024, 2013.

469 Bond-Lamberty, B., Peckham, S. D., Ahl, D. E., and Gower, S. T.: Fire as the dominant driver of
470 central Canadian boreal forest carbon balance, *Nature*, 450, 89-92, 10.1038/nature06272, 2007.

471 Bond-Lamberty, B., and Thomson, A.: Temperature-associated increases in the global soil
472 respiration record, *Nature*, 464, 579-582, 10.1038/nature08930, 2010.

473 Callaghan, T., Björn, L. O., Chernov, Y., Chapin, T., Christensen, T. R., Huntley, B., Ims, R.,
474 Jolly, D., Jonasson, S., Matveyeva, N., Panikov, N., Oechel, W., and Shaver, G.: Arctic tundra
475 and polar desert ecosystems, *Arctic climate impact assessment*, 243-352, 2005.

476 Chapin, F. S., and Starfield, A. M.: Time lags and novel ecosystems in response to transient
477 climatic change in arctic Alaska, *Climatic change*, 35, 449-461, 1997.

478 Christensen, J. H., and Christensen, O. B.: A summary of the PRUDENCE model projections of
479 changes in European climate by the end of this century, *Climatic Change*, 81, 7-30,
480 10.1007/s10584-006-9210-7, 2007.

481 Ciais, P., Sabine, C., Bala, G., Bopp, L., Brovkin, V., Canadell, J., Chhabra, A., DeFries, R.,
482 Galloway, J., Heimann, M., Jones, C., Quéré, C. L., Myneni, R. B., Piao, S., and Thornton, P.:
483 Carbon and other biogeochemical cycles, *Climate change 2013: the physical science basis*.
484 Contribution of Working Group I to the Fifth Assessment Report of the Intergovernmental Panel
485 on Climate Change, 465-570, 2014.

486 Cole, C. V., Duxbury, J., Freney, J., Heinemeyer, O., K. Minami, Mosier, A., Paustian, K.,
487 Rosenberg, N., Sampson, N., Sauerbeck, D., and Zhao, Q.: Global estimates of potential
488 mitigation of greenhouse gas emissions by agriculture, *Nutrient cycling in Agroecosystems*, 49,
489 221-228, 1997.

490 Davidson, E. A., Trumbore, S. E., and Amundson, R.: Biogeochemistry: soil warming and
491 organic carbon content, *Nature*, 408, 2000.

492 Davidson, E. A., and Janssens, I. A.: Temperature sensitivity of soil carbon decomposition and
493 feedbacks to climate change, *Nature*, 440, 165-173, 10.1038/nature04514, 2006.

494 Dong, Y., and Somero, G. N.: Temperature adaptation of cytosolic malate dehydrogenases of
495 limpets (genus *Lottia*): differences in stability and function due to minor changes in sequence
496 correlate with biogeographic and vertical distributions, *The Journal of experimental biology*, 212,
497 169-177, 10.1242/jeb.024505, 2009.

498 Duan, Q., Sorooshian, S., and Gupta, V. K.: Optimal use of the SCE-UA global optimization
499 method for calibrating watershed models, *Journal of Hydrology*, 158, 265-284, 1994.

500 Esteban G. Jobbág, and Jackson, R. B.: The vertical distribution of soil organic carbon and its
501 relation to climate and vegetation, *Ecological applications*, 10, 423-436, 2000.

502 Gear, A. J., and Huntley, B.: Rapid changes in the range limits of Scots pine 4000 years ago,
503 Science, 251, 544-547, 1991.

504 German, D. P., Marcelo, K. R. B., Stone, M. M., and Allison, S. D.: The Michaelis-Menten
505 kinetics of soil extracellular enzymes in response to temperature: a cross-latitudinal study,
506 Global change biology, 18, 1468-1479, 10.1111/j.1365-2486.2011.02615.x, 2012.

507 Goetz, S. J., Mack, M. C., Gurney, K. R., Randerson, J. T., and Houghton, R. A.: Ecosystem
508 responses to recent climate change and fire disturbance at northern high latitudes: observations
509 and model results contrasting northern Eurasia and North America, Environmental Research
510 Letters, 2, 045031, 10.1088/1748-9326/2/4/045031, 2007.

511 Hagerty, S. B., van Groenigen, K. J., Allison, S. D., Hungate, B. A., Schwartz, E., Koch, G. W.,
512 Kolka, R. K., and Dijkstra, P.: Accelerated microbial turnover but constant growth efficiency
513 with warming in soil, Nature Climate Change, 4, 903-906, 10.1038/nclimate2361, 2014.

514 Hansen, J., Sato, M., Ruedy, R., Lo, K., Lea, D. W., and Medina-Elizade, M.: Global
515 temperature change, Proceedings of the National Academy of Sciences of the United States of
516 America, 103, 14288-14293, 10.1073/pnas.0606291103, 2006.

517 Hanson, P. J., Edwards, N. T., Garten, C. T., and Andrews, J. A.: Separating root and soil
518 microbial contributions to soil respiration: A review of methods and observations,
519 Biogeochemistry, 48, 115-146, 2000.

520 Hao, G., Zhuang, Q., Zhu, Q., He, Y., Jin, Z., and Shen, W.: Quantifying microbial
521 ecophysiological effects on the carbon fluxes of forest ecosystems over the conterminous United
522 States, Climatic Change, 133, 695-708, 10.1007/s10584-015-1490-3, 2015.

523 Harden, J. W., Trumbore, S. E., Stocks, B. J., Hirsch, A., Gower, S. T., O'Neill, K. P., and
524 Kasischke, E. S.: The role of fire in the boreal carbon budget, Global change biology, 6, 174-184,
525 2000.

526 Harris, I., Jones, P. D., Osborn, T. J., and Lister, D. H.: Updated high-resolution grids of monthly
527 climatic observations - the CRU TS3.10 Dataset, International Journal of Climatology, 34, 623-
528 642, 10.1002/joc.3711, 2014.

529 Hayes, D. J., Kicklighter, D. W., McGuire, A. D., Chen, M., Zhuang, Q., Yuan, F., Melillo, J. M.,
530 and Wullschleger, S. D.: The impacts of recent permafrost thaw on land-atmosphere greenhouse
531 gas exchange, Environmental Research Letters, 9, 045005, 10.1088/1748-9326/9/4/045005, 2014.

532 He, Y., Yang, J., Zhuang, Q., Harden, J. W., McGuire, A. D., Liu, Y., Wang, G., and Gu, L.:
533 Incorporating microbial dormancy dynamics into soil decomposition models to improve
534 quantification of soil carbon dynamics of northern temperate forests, Journal of Geophysical
535 Research: Biogeosciences, 120, 2596-2611, 10.1002/2015jg003130, 2015.

536 Hobbie, E. A., and Hobbie, J. E.: Natural Abundance of 15N in Nitrogen-Limited Forests and
537 Tundra Can Estimate Nitrogen Cycling Through Mycorrhizal Fungi: A Review, Ecosystems, 11,
538 815-830, 10.1007/s10021-008-9159-7, 2008.

539 Hobbie, J. E., and Hobbie, E. A.: 15N in symbiotic fungi and plants estimates nitrogen and
540 carbon flux rates in Arctic tundra, Ecology, 87, 816-822, 2006.

541 Holland, M. M., and Bitz, C. M.: Polar amplification of climate change in coupled models,
542 Climate Dynamics, 21, 221-232, 10.1007/s00382-003-0332-6, 2003.

543 Houghton, R. A.: Balancing the Global Carbon Budget, Annual Review of Earth and Planetary
544 Sciences, 35, 313-347, 10.1146/annurev.earth.35.031306.140057, 2007.

545 Johnstone, J. F., and Kasischke, E. S.: Stand-level effects of soil burn severity on postfire
546 regeneration in a recently burned black spruce forest, *Canadian Journal of Forest Research*, 35,
547 2151-2163, 10.1139/x05-087, 2005.

548 Kasischke, E. S., and Turetsky, M. R.: Recent changes in the fire regime across the North
549 American boreal region—Spatial and temporal patterns of burning across Canada and Alaska,
550 *Geophysical Research Letters*, 33, 10.1029/2006gl025677, 2006.

551 Knorr, W.: Annual and interannual CO₂ exchanges of the terrestrial biosphere: process-based
552 simulations and uncertainties, *Global Ecology and Biogeography*, 9, 225-252, 2000.

553 Lawrence, D. M., Oleson, K. W., Flanner, M. G., Thornton, P. E., Swenson, S. C., Lawrence, P.
554 J., Zeng, X., Yang, Z.-L., Levis, S., Sakaguchi, K., Bonan, G. B., and Slater, A. G.:
555 Parameterization improvements and functional and structural advances in Version 4 of the
556 Community Land Model, *Journal of Advances in Modeling Earth Systems*, 3,
557 10.1029/2011ms000045, 2011.

558 Lennon, J. T., and Jones, S. E.: Microbial seed banks: the ecological and evolutionary
559 implications of dormancy, *Nature reviews. Microbiology*, 9, 119-130, 10.1038/nrmicro2504,
560 2011.

561 Lloyd, A. H.: Ecological histories from Alaskan tree lines provide insight into future change,
562 *Ecology*, 86, 1687-1695, 2005.

563 Mack, M. C., Schuur, E. A. G., Bret-Harte, M. S., Shaver, G. R., and III, F. S. C.: Ecosystem
564 carbon storage in arctic tundra reduced by long-term nutrient fertilization, *Nature*, 431, 2004.

565 McGuire, A. D., Melillo, J. M., Joyce, L. A., Kicklighter, D. W., Grace, A. L., III, B. M., and
566 Vorosmarty, C. J.: Interactions between carbon and nitrogen dynamics in estimating net primary
567 productivity for potential vegetation in North America, *Global Biogeochemical Cycles*, 6, 101-
568 124, 1992.

569 McGuire, A. D., Melillo, J. M., Kicklighter, D. W., and Joyce, L. A.: Equilibrium responses of
570 soil carbon to climate change: Empirical and process-based estimates, *Journal of Biogeography*,
571 785-796, 1995.

572 McGuire, A. D., and Hobbie, J. E.: Global climate change and the equilibrium responses of
573 carbon storage in arctic and subarctic regions, In *Modeling the Arctic system: A workshop report*
574 on the state of modeling in the Arctic System Science program, 53-54, 1997.

575 McGuire, A. D., Anderson, L. G., Christensen, T. R., Dallimore, S., Guo, L., Hayes, D. J.,
576 Heimann, M., Lorensen, T. D., Macdonald, R. W., and Roulet, N.: Sensitivity of the carbon
577 cycle in the Arctic to climate change, *Ecological Monographs*, 79, 523-555, 2009.

578 McGuire, A. D., Christensen, T. R., Hayes, D., Heroult, A., Euskirchen, E., Kimball, J. S.,
579 Koven, C., Lafleur, P., Miller, P. A., Oechel, W., Peylin, P., Williams, M., and Yi, Y.: An
580 assessment of the carbon balance of Arctic tundra: comparisons among observations, process
581 models, and atmospheric inversions, *Biogeosciences*, 9, 3185-3204, 10.5194/bg-9-3185-2012,
582 2012.

583 Melillo, J. M., McGuire, A. D., Kicklighter, D. W., III, B. M., Vorosmarty, C. J., and Schloss, A.
584 L.: Global climate change and terrestrial net primary production, *Nature*, 363, 1993.

585 Oechel, W. C., Vourlitis, G. L., Hastings, S. J., Zulueta, R. C., Hinzman, L., and Kane, D.:
586 Acclimation of ecosystem CO₂ exchange in the Alaskan Arctic in response to decadal climate
587 warming, *Nature*, 406, 978, 2000.

588 Orchard, V. A., and Cook, F. J.: Relationship between soil respiration and soil moisture, 15, 447-
589 453, 1983.

590 Parton, W. J., Ojima, D. S., Cole, C. V., and Schimel, D. S.: A general model for soil organic
591 matter dynamics: sensitivity to litter chemistry, texture and management, Quantitative modeling
592 of soil forming processes, 147-167, 1994.

593 Potter, C. S., Randerson, J. T., Field, C. B., Matson, P. A., Vitousek, P. M., Mooney, H. A., and
594 Klooster, S. A.: Terrestrial ecosystem production: a process model based on global satellite and
595 surface data, *Global Biogeochemical Cycles*, 7, 811-841, 1993.

596 Qian, H., Joseph, R., and Zeng, N.: Enhanced terrestrial carbon uptake in the Northern High
597 Latitudes in the 21st century from the Coupled Carbon Cycle Climate Model Intercomparison
598 Project model projections, *Global change biology*, 16, 641-656, 10.1111/j.1365-
599 2486.2009.01989.x, 2010.

600 Raich, J. W., and Schlesinger, W. H.: The global carbon dioxide flux in soil respiration and its
601 relationship to vegetation and climate, *Tellus B*, 44, 81-99, 1992.

602 Randerson, J. T., Liu, H., Flanner, M. G., Chambers, S. D., Jin, Y., Hess, P. G., Pfister, G., Mack,
603 M. C., Treseder, K. K., Welp, L. R., Chapin, F. S., Harden, J. W., Goulden, M. L., Lyons, E.,
604 Neff, J. C., Schuur, E. A. G., and Zender, C. S.: The impact of boreal forest fire on climate
605 warming, *science*, 1130-1132, 2006.

606 Running, S. W., and Coughlan, J. C.: A general model of forest ecosystem processes for regional
607 applications I. Hydrologic balance, canopy gas exchange and primary production processes.,
608 *Ecological Modelling*, 42, 125-154, 1988.

609 Schaphoff, S., Heyder, U., Ostberg, S., Gerten, D., Heinke, J., and Lucht, W.: Contribution of
610 permafrost soils to the global carbon budget, *Environmental Research Letters*, 8, 014026,
611 10.1088/1748-9326/8/1/014026, 2013.

612 Schimel, J.: The implications of exoenzyme activity on microbial carbon and nitrogen limitation
613 in soil: a theoretical model, *Soil Biology and Biochemistry*, 35, 549-563, 10.1016/s0038-
614 0717(03)00015-4, 2003.

615 Schimel, J.: Microbes and global carbon, *Nature Climate Change*, 3, 867-868,
616 10.1038/nclimate2015, 2013.

617 Schimel, J. P., and Hättenschwiler, S.: Nitrogen transfer between decomposing leaves of
618 different N status, *Soil Biology and Biochemistry*, 39, 1428-1436, 10.1016/j.soilbio.2006.12.037,
619 2007.

620 Schimel, J. P., and Schaeffer, S. M.: Microbial control over carbon cycling in soil, *Frontiers in
621 microbiology*, 3, 348, 10.3389/fmicb.2012.00348, 2012.

622 Schmidt, M. W., Torn, M. S., Abiven, S., Dittmar, T., Guggenberger, G., Janssens, I. A., Kleber,
623 M., Kogel-Knabner, I., Lehmann, J., Manning, D. A., Nannipieri, P., Rasse, D. P., Weiner, S.,
624 and Trumbore, S. E.: Persistence of soil organic matter as an ecosystem property, *Nature*, 478,
625 49-56, 10.1038/nature10386, 2011.

626 Schuur, E. A. G., Bockheim, J., Canadell, J. G., Euskirchen, E., Field, C. B., Goryachkin, S. V.,
627 Hagemann, S., Kuhry, P., Lafleur, P. M., Lee, H., and Mazhitova, G.: Vulnerability of
628 permafrost carbon to climate change: Implications for the global carbon cycle, *BioScience*, 58,
629 701-714, 2008.

630 Serreze, M. C., and Francis, J. A.: The Arctic on the fast track of change, *Weather*, 61, 65-69,
631 2006.

632 Soja, A. J., Tchebakova, N. M., French, N. H. F., Flannigan, M. D., Shugart, H. H., Stocks, B. J.,
633 Sukhinin, A. I., Parfenova, E. I., Chapin, F. S., and Stackhouse, P. W.: Climate-induced boreal
634 forest change: Predictions versus current observations, *Global and Planetary Change*, 56, 274-
635 296, 10.1016/j.gloplacha.2006.07.028, 2007.

636 Somero, G. N.: Adaptation of enzymes to temperature: searching for basic "strategies",
637 Comparative biochemistry and physiology. Part B, *Biochemistry & molecular biology*, 139, 321-
638 333, 10.1016/j.cbpc.2004.05.003, 2004.

639 Steinweg, J. M., Plante, A. F., Conant, R. T., Paul, E. A., and Tanaka, D. L.: Patterns of substrate
640 utilization during long-term incubations at different temperatures, *Soil Biology and Biochemistry*,
641 40, 2722-2728, 10.1016/j.soilbio.2008.07.002, 2008.

642 Steinweg, J. M., Dukes, J. S., Paul, E. A., and Wallenstein, M. D.: Microbial responses to multi-
643 factor climate change: effects on soil enzymes, *Frontiers in microbiology*, 4, 146,
644 10.3389/fmicb.2013.00146, 2013.

645 Stone, M. M., Weiss, M. S., Goodale, C. L., Adams, M. B., Fernandez, I. J., German, D. P., and
646 Allison, S. D.: Temperature sensitivity of soil enzyme kinetics under N-fertilization in two
647 temperate forests, *Global change biology*, 18, 1173-1184, 10.1111/j.1365-2486.2011.02545.x,
648 2012.

649 Stow, D. A., Hope, A., McGuire, D., Verbyla, D., Gamon, J., Huemmrich, F., Houston, S.,
650 Racine, C., Sturm, M., Tape, K., Hinzman, L., Yoshikawa, K., Tweedie, C., Noyle, B.,
651 Silapaswan, C., Douglas, D., Griffith, B., Jia, G., Epstein, H., Walker, D., Daeschner, S.,
652 Petersen, A., Zhou, L., and Myneni, R.: Remote sensing of vegetation and land-cover change in
653 Arctic Tundra Ecosystems, *Remote Sensing of Environment*, 89, 281-308,
654 10.1016/j.rse.2003.10.018, 2004.

655 Sturm, M., Racine, C., and Tape, K.: Climate change: increasing shrub abundance in the Arctic.,
656 *Nature*, 411, 2001.

657 Tang, J., and Zhuang, Q.: Equifinality in parameterization of process-based biogeochemistry
658 models: A significant uncertainty source to the estimation of regional carbon dynamics, *Journal*
659 *of Geophysical Research: Biogeosciences*, 113, 10.1029/2008jg000757, 2008.

660 Tape, K. E. N., Sturm, M., and Racine, C.: The evidence for shrub expansion in Northern Alaska
661 and the Pan-Arctic, *Global change biology*, 12, 686-702, 10.1111/j.1365-2486.2006.01128.x,
662 2006.

663 Tarnocai, C., Canadell, J. G., Schuur, E. A. G., Kuhry, P., Mazhitova, G., and Zimov, S.: Soil
664 organic carbon pools in the northern circumpolar permafrost region, *Global Biogeochemical*
665 *Cycles*, 23, n/a-n/a, 10.1029/2008gb003327, 2009.

666 Todd-Brown, K. E. O., Hopkins, F. M., Kivlin, S. N., Talbot, J. M., and Allison, S. D.: A
667 framework for representing microbial decomposition in coupled climate models,
668 *Biogeochemistry*, 109, 19-33, 10.1007/s10533-011-9635-6, 2011.

669 Todd-Brown, K. E. O., Randerson, J. T., Post, W. M., Hoffman, F. M., Tarnocai, C., Schuur, E.
670 A. G., and Allison, S. D.: Causes of variation in soil carbon simulations from CMIP5 Earth
671 system models and comparison with observations, *Biogeosciences*, 10, 1717-1736, 10.5194/bg-
672 10-1717-2013, 2013.

673 White, A., Cannell, M. G. R., and Friend, A. D.: The high-latitude terrestrial carbon sink: a
674 model analysis *Global change biology*, 6, 227-245, 2000.

675 Wieder, W. R., Bonan, G. B., and Allison, S. D.: Global soil carbon projections are improved by
676 modelling microbial processes, *Nature Climate Change*, 3, 909-912, 10.1038/nclimate1951, 2013.
677 Zhuang, Q., Romanovsky, V. E., and McGuire, A. D.: Incorporation of a permafrost model into a
678 large-scale ecosystem model: Evaluation of temporal and spatial scaling issues in simulating soil
679 thermal dynamics, *Journal of Geophysical Research: Atmospheres*, 106, 33649-33670,
680 10.1029/2001jd900151, 2001.
681 Zhuang, Q., McGuire, A. D., O'Neill, K. P., Harden, J. W., Romanovsky, V. E., and Yarie, J.:
682 Modeling soil thermal and carbon dynamics of a fire chronosequence in interior Alaska, *Journal*
683 of *Geophysical Research*, 108, 10.1029/2001jd001244, 2002.
684 Zhuang, Q., He, J., Lu, Y., Ji, L., Xiao, J., and Luo, T.: Carbon dynamics of terrestrial
685 ecosystems on the Tibetan Plateau during the 20th century: an analysis with a process-based
686 biogeochemical model, *Global Ecology and Biogeography*, no-no, 10.1111/j.1466-
687 8238.2010.00559.x, 2010.
688 Zhuang, Q., Chen, M., Xu, K., Tang, J., Saikawa, E., Lu, Y., Melillo, J. M., Prinn, R. G., and
689 McGuire, A. D.: Response of global soil consumption of atmospheric methane to changes in
690 atmospheric climate and nitrogen deposition, *Global Biogeochemical Cycles*, 27, 650-663,
691 10.1002/gbc.20057, 2013.
692 Zhuang, Q., Zhu, X., He, Y., Prigent, C., Melillo, J. M., David McGuire, A., Prinn, R. G., and
693 Kicklighter, D. W.: Influence of changes in wetland inundation extent on net fluxes of carbon
694 dioxide and methane in northern high latitudes from 1993 to 2004, *Environmental Research*
695 *Letters*, 10, 095009, 10.1088/1748-9326/10/9/095009, 2015.
696 Zhuang, Q., McGuire, A. D., Melillo, J. M., Clein, J. S., Dargaville, R. J., Kicklighter, D. W.,
697 Myneni, R. B., Dong, J., Romanovsky, V. E., Harden, J., and Hobbie, J. E.: Carbon cycling in
698 extratropical terrestrial ecosystems of the Northern Hemisphere during the 20th century: a
699 modeling analysis of the influences of soil thermal dynamics, *Tellus B: Chemical and Physical*
700 *Meteorology*, 55, 751-776, 10.3402/tellusb.v55i3.16368, 2003.
701 Zimov, S. A., Schuur, E. A. G., and III, F. S. C.: Permafrost and the global carbon budget,
702 *Science*, 312, 1612-1613, 2006.

703

704

705 **Author contributions.** Q.Z. designed the study. J.Z. conducted model development, simulation
706 and analysis. J.Z. and Q. Z. wrote the paper.

707

708 **Competing financial interests.** The submission has no competing financial interests.

709

710 **Materials & Correspondence.** Correspondence and material requests should be addressed to
711 qzhuang@purdue.edu.

712

713

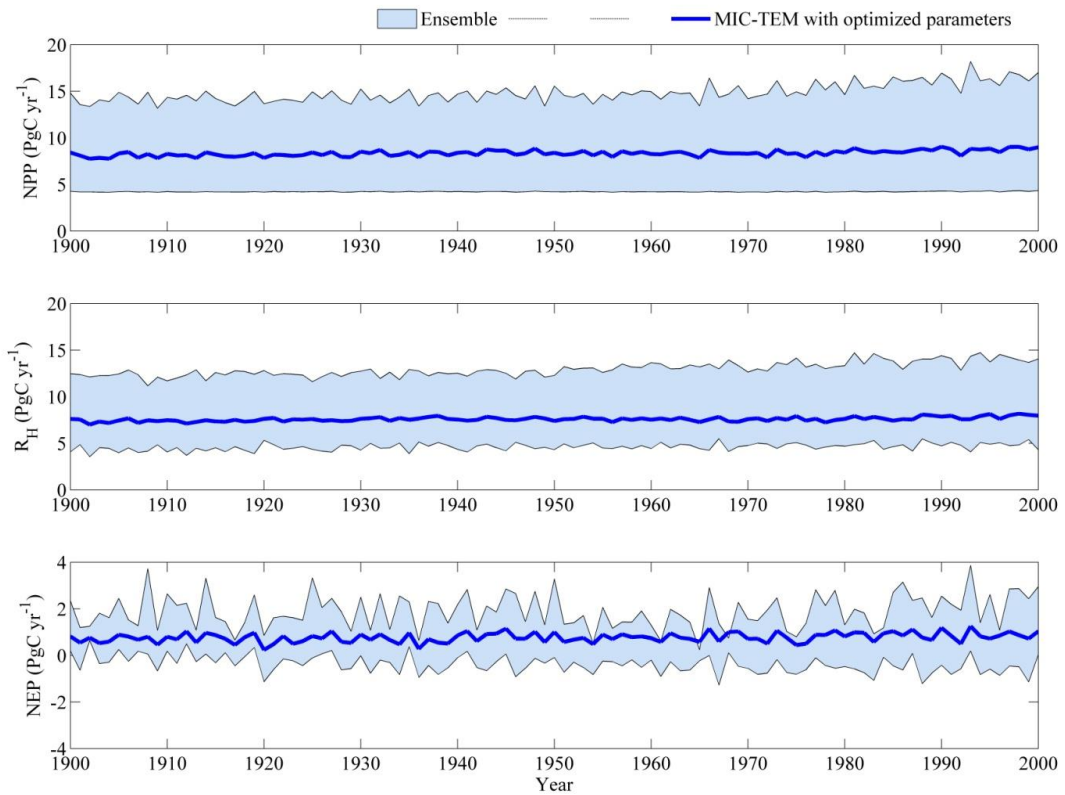


Figure 1. Simulated annual net primary production (NPP, top panel), heterotrophic respiration (R_H , center panel) and net ecosystem production (NEP, bottom panel) by MIC-TEM with ensemble of parameters.

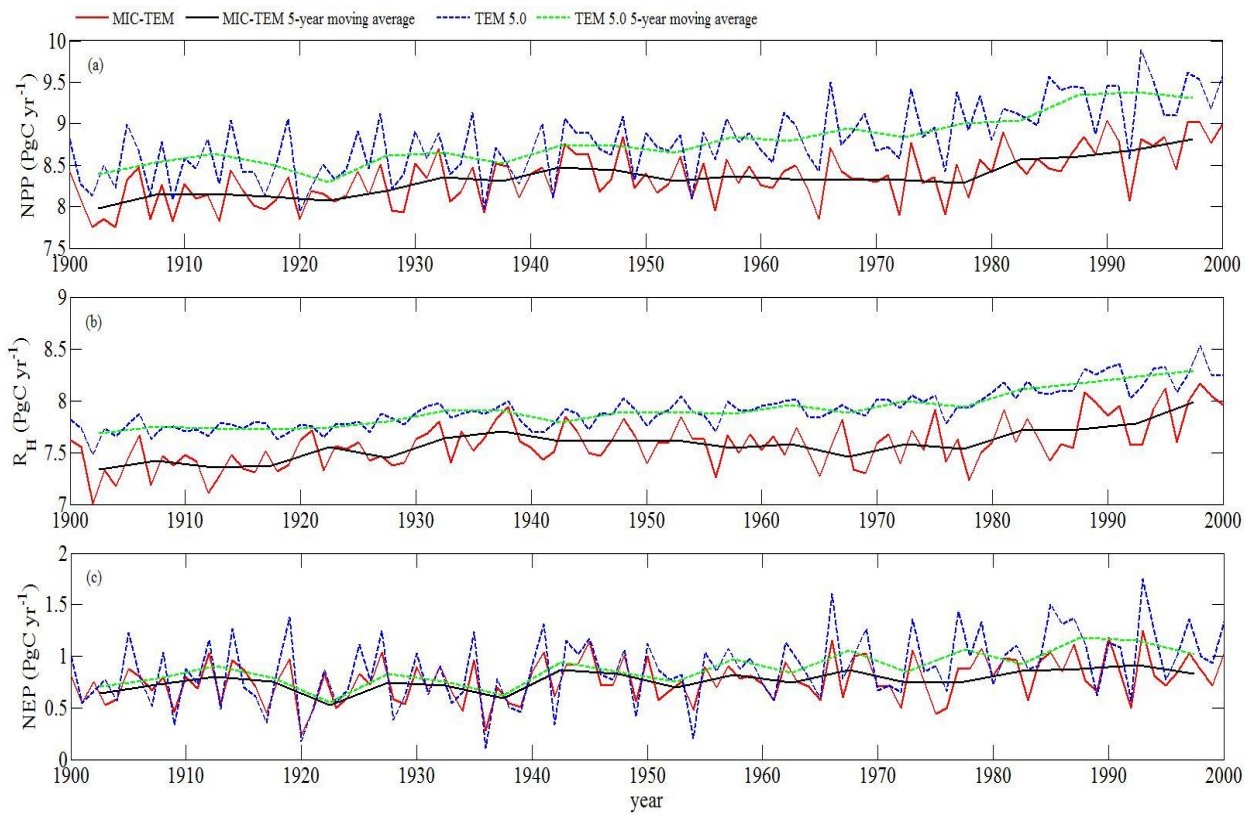


Figure 2. Simulated annual net primary production (NPP, top panel), heterotrophic respiration (R_H , center panel) and net ecosystem production (NEP, bottom panel) by MIC-TEM and TEM, respectively.

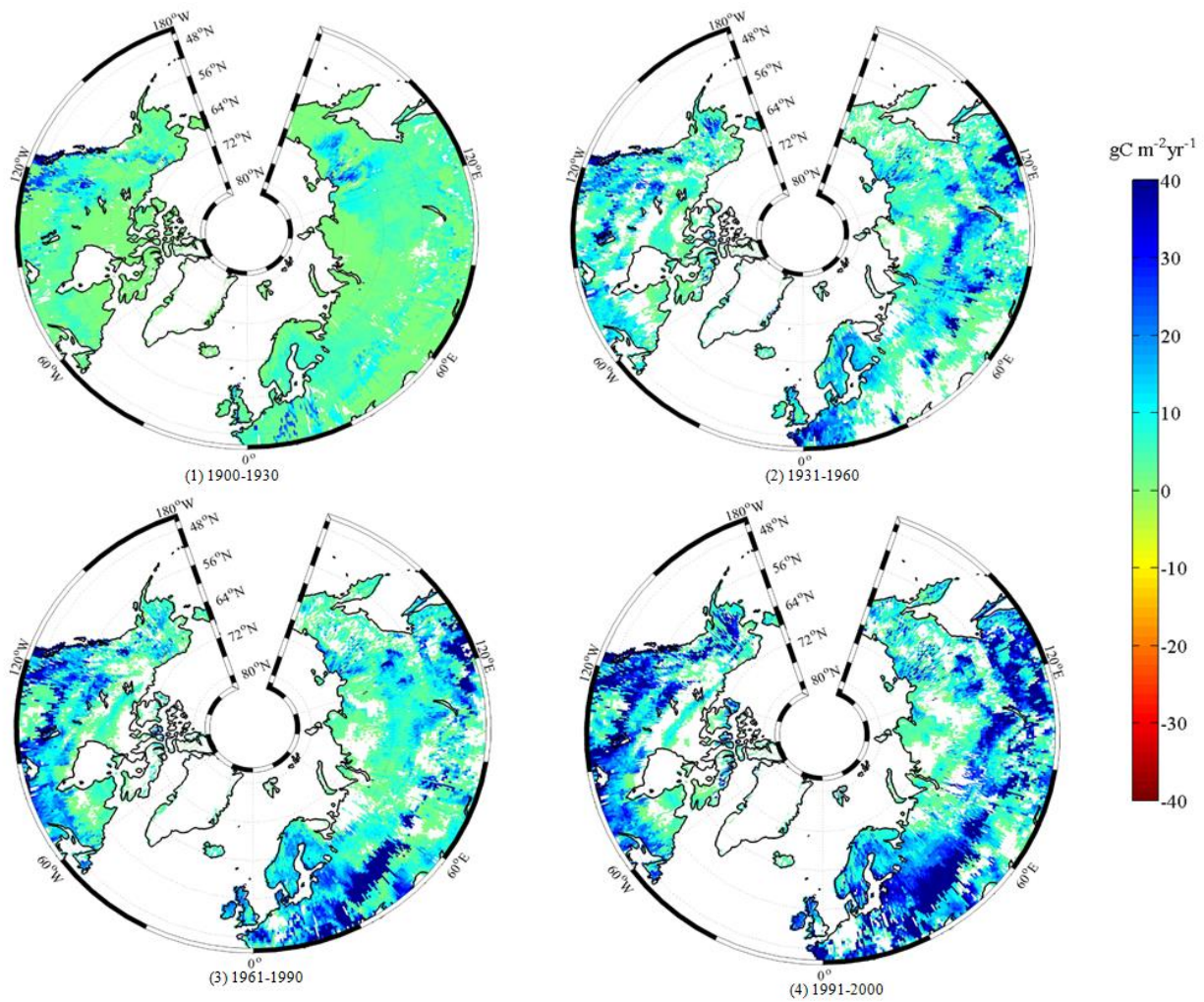


Figure 3. Spatial distribution of NEP simulated by MIC-TEM for the periods: (1) 1900-1930, (2) 1931-1960, (3) 1961-1990, and (4) 1991-2000. Positive values of NEP represent sinks of CO_2 into terrestrial ecosystems, while negative values represent sources of CO_2 to the atmosphere.

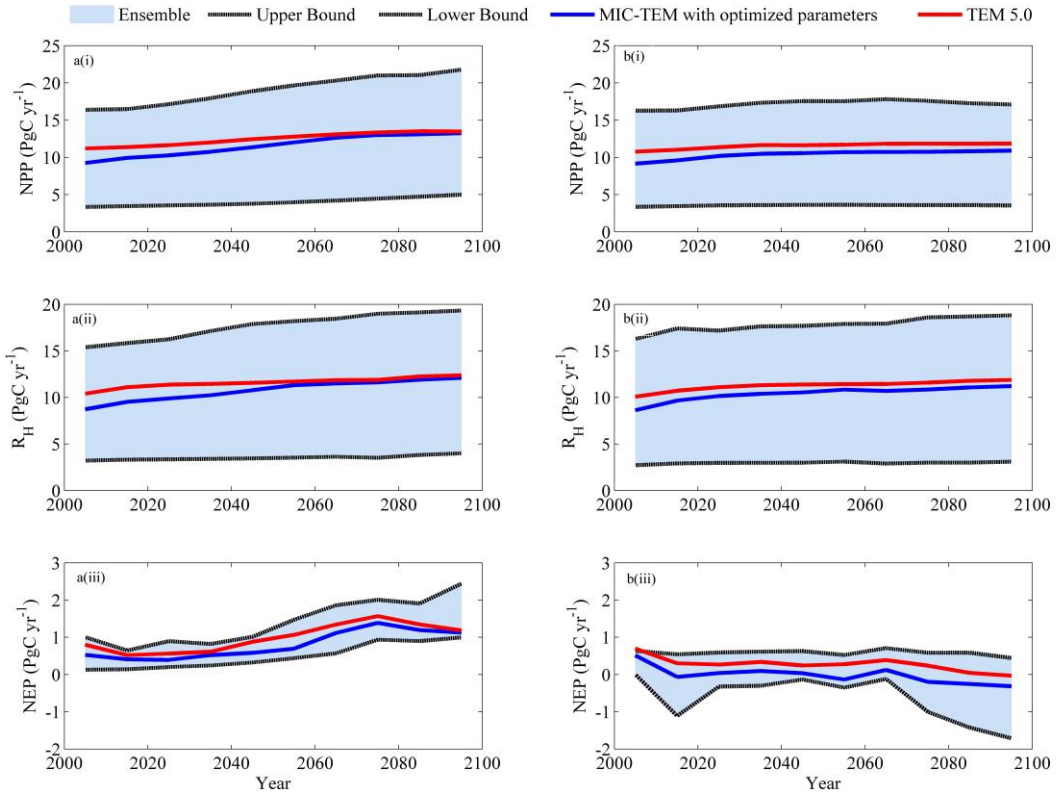


Figure 4. Predicted changes in carbon fluxes: (i) NPP, (ii) R_H , and (iii) NEP for all land areas north of 45 °N in response to transient climate change under (a) RCP 8.5 scenario and (b) RCP 2.6 scenario with MIC-TEM and TEM 5.0, respectively. The decadal running mean is applied. The grey area represents the upper and lower bounds of simulations.

Table 1. Parameters associated with more detailed microbial dynamics in MIC-TEM

Process	Parameter	Units	Initial Value	Description	Parameter range	Reference
Assimilation	$Vmax_{uptake_0}$	mg DOC cm ⁻³ (mg biomass cm ⁻³) ⁻¹ h ⁻¹	9.97e6	Maximum microbial uptake rate	[1.0e4, 1.0e8]	Hao et al. (2015)
	Ea_{uptake}	kJ mol ⁻¹	47	Activation energy	-	Allison et al. (2010)
	$Km_{uptake_{slope}}$	mg cm ⁻³ degree ⁻¹	0.01	Temperature regulator of MM for DOC uptake by microbes	-	Allison et al. (2010)
	Km_{uptake_0}	mg cm ⁻³	0.1	Temperature regulator of MM for DOC uptake by microbes	-	Allison et al. (2010)
CO ₂ production	CUE_{slope}	degree ⁻¹	-0.016	Temperature regulator of carbon use efficiency	-	Allison et al. (2010)
	CUE_0	-	0.63	Temperature regulator of carbon use efficiency	-	Allison et al. (2010)
Decay	$Vmax_0$	mg SOC cm ⁻³ (mg Enz cm ⁻³) ⁻¹ h ⁻¹	9.17e7	Maximum rate of converting SOC to soluble C	[1.0e5, 1.0e8]	Hao et al. (2015)
	Ea	kJ mol ⁻¹	47	Activation energy	-	Allison et al. (2010)
	Km_{slope}	mg cm ⁻³ degree ⁻¹	5	Temperature regulator of MM for enzymatic decay	-	Allison et al. (2010)
	Km_0	mg cm ⁻³	500	Temperature regulator of MM for enzymatic decay	-	Allison et al. (2010)
MIC turnover	r_{death}	s ⁻¹	0.02	Microbial death fraction	-	Allison et al. (2010)
	MICtoSOC		50	Partition coefficient for dead microbial biomass between the SOC and DOC pool	-	Allison et al. (2010)
ENZ turnover	$r_{EnzProd}$	s ⁻¹	5.0e-4	Enzyme production fraction	-	Allison et al. (2010)
	$r_{EnzLoss}$	s ⁻¹	0.1	Enzyme loss fraction	-	Allison et al. (2010)

Table 2. Partitioning of average annual net ecosystem production (as Pg C per year) for six vegetation types during the 20th century

	MIC-TEM (PgC yr ⁻¹)	TEM 5.0 (PgC yr ⁻¹)
Alpine tundra	0.03	0.04
Boreal forest	0.39	0.45
Conifer forest	0.09	0.09
Deciduous forest	0.16	0.18
Grassland	0.06	0.07
Wet tundra	0.05	0.06
Total	0.78	0.89

Table 3. Increasing of SOC, vegetation carbon (VGC), soil organic nitrogen (SON), vegetation nitrogen (VGN) from 1900 to 2000, and total carbon storage during the 21st century predicted by two models with observed soil carbon data of three different depths under (a) RCP 2.6 and (b) RCP 8.5.

(a)

Model	Units: Pg	Without (control)	30cm	100cm	300cm
TEM 5.0	SOC/SON in 2000	604.2/27.0	429.5/19.0	689.3/31.6	1003.4/46.2
	Increase of SOC during the 21 st century	12.1	9.9	16.0	22.8
	VGC/VGN in 2000	318.3/1.48	238.4/1.05	394.2/1.80	556.7/2.53
	Increase of VGC during the 21 st century	15.5	10.5	18.0	25.3
	Increase of total carbon storage during the 21 st century	27.6	20.4	34.0	48.1
	SOC/SON in 2000	591.5/26.8	420.3/18.6	686.0/31.2	990.7/45.3
MIC-TEM	Increase of SOC during the 21 st century	-2.0	-1.2	-2.4	-2.9
	VGC/VGN in 2000	309.7/1.42	230.1/1.02	374.4/1.71	548.6/2.45
	Increase of VGC during the 21 st century	0.4	0.5	0.2	-0.1
	Increase of total carbon storage during the 21 st century	-1.6	-0.7	-2.2	-3.0

(b)

Model	Units: Pg	Without (control)	30cm	100cm	300cm
TEM 5.0	SOC/SON in 2000	610.2 /27.9	431.9/19.1	693.8/31.8	1007.1/46.4
	Increase of SOC during the 21 st century	44.2	33.0	56.5	74.6
	VGC/VGN in 2000	324.9/1.50	242.1/1.07	399.6/1.83	570.2/2.57
	Increase of VGC during the 21 st century	54.5	38.7	63.5	81.0
	Increase of total carbon storage during the 21 st century	98.7	71.7	120.0	155.6
	SOC/SON in 2000	596.0/27.1	424.6/18.8	689.1/31.5	995.5/46.1
MIC-TEM	Increase of SOC during the 21 st century	33.3	27.4	36.9	42.9
	VGC/VGN in 2000	316.0/1.44	233.5/1.02	380.0/1.72	568.3/2.56
	Increase of VGC during the 21 st century	46.2	37.0	51.7	56.9
	Increase of total carbon storage during the 21 st century	79.5	65.4	88.6	109.8